Electronic Supplementary Information

Low-temperature crystallography and vibrational properties of rozenite ($FeSO_4·4H_2O$), a candidate mineral component of the polyhydrated sulfate deposits on Mars

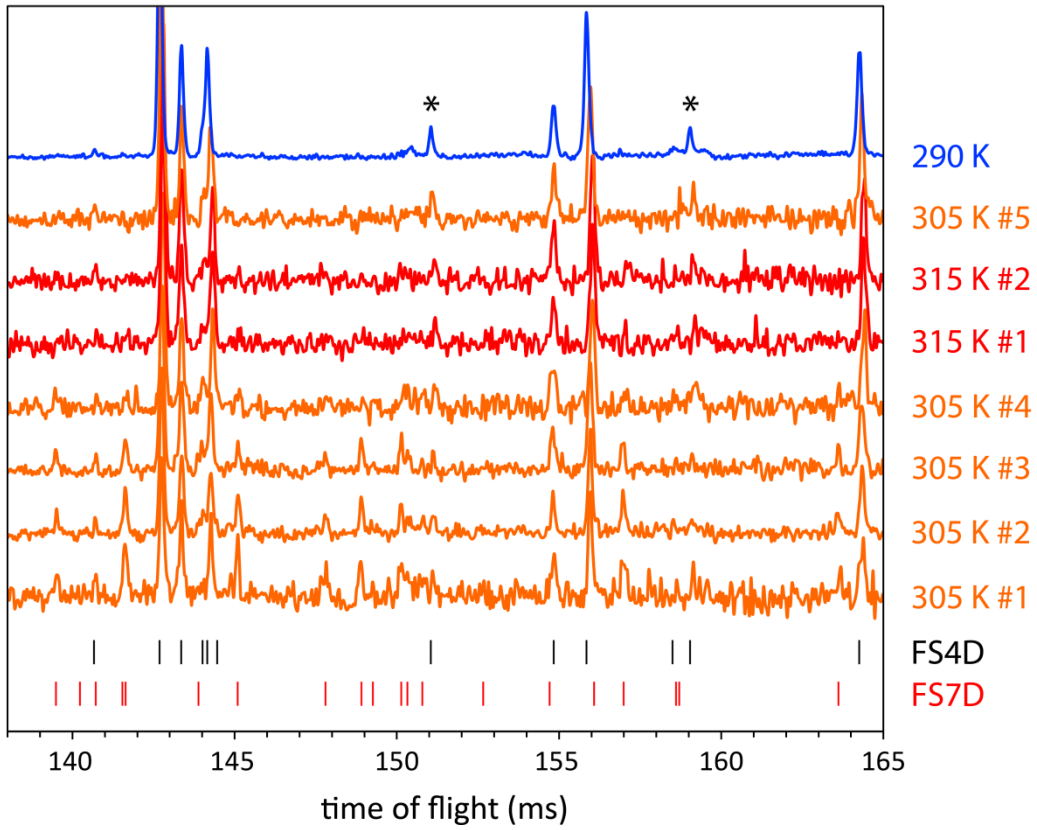

Fig. S1. Stack plot of neutron powder diffraction data collected after the initial sample loading. Data was collected sequentially at 305 K (#1 for 8 min; #2 for 28 m; #3 for 22 m; #4 for 10 m) revealing the presence of a small amount of $FeSO_4·7D_2O$ (FS7D, red tick marks) in addition to $FeSO_4·4D_2O$ (FS4D, black tick marks), which represents the bulk of the sample. Data were then collected at 315 K (#1 for 10 min; #2 for another 10 m) to confirm elimination of the FS7D phase. However small peaks from $FeSO_4·D_2O$ (asterisks) appeared at this temperature, persisting on cooling back to 305 K (#5) and at 290 K.

rozenite - bond valence - without hydrogen									
	O1	O2	O3	O4	Ow1	Ow2	Ow3	Ow4	Σ
Fe - O	0.349	0.341			0.375	0.336	0.361	0.375	2.137
S - O	1.554	1.558	1.600	1.545					6.257
Σ	1.903	1.899	1.600	1.545	0.375	0.336	0.361	0.375	

rozenite - bond valence - with hydrogen									
	O1	O2	O3	O4	Ow1	Ow2	Ow3	Ow4	Σ
Fe - O	0.349	0.341			0.375	0.336	0.361	0.375	2.137
S - O	1.554	1.558	1.600	1.545					6.257
O - H					1.814	1.814	1.841	1.783	7.253
H ···									
O	0.093	0.048	0.306	0.204				0.017	
Σ	1.996	1.946	1.906	1.749	2.189	2.150	2.202	2.175	

Table S1. Bond valance calculations for rozenite excluding (top) and including (bottom) the contribution of the hydrogen atoms (bottom). For the Fe – O and S – O bonds a universal parameter of 0.37 as suggested by Brown & Altermatt (1985) was used, whereas the O – H and H ··· O values were computed using a more recent universal parameter of 0.404 as derived by Alig et al. (1994) specifically for hydrogen bonds. r_0 values for Fe – O (1.734) and S – O (1.644) were taken from Brese & O'Keeffe (1991) and for O – H (0.914) from Alig et al. (1994). Note that inclusion of the H2b ::: O2/O2' contact substantially improves the bond valance calculation. The Ow atoms are systematically oversaturated by 0.15 – 0.20 valence units, thus the inclusion of the H3a ••• Ow4 contact into the calculation does not improve the calculation. However, based on geometrical considerations it is evident that the H3a ••• Ow4 contact forms a weak hydrogen bond.

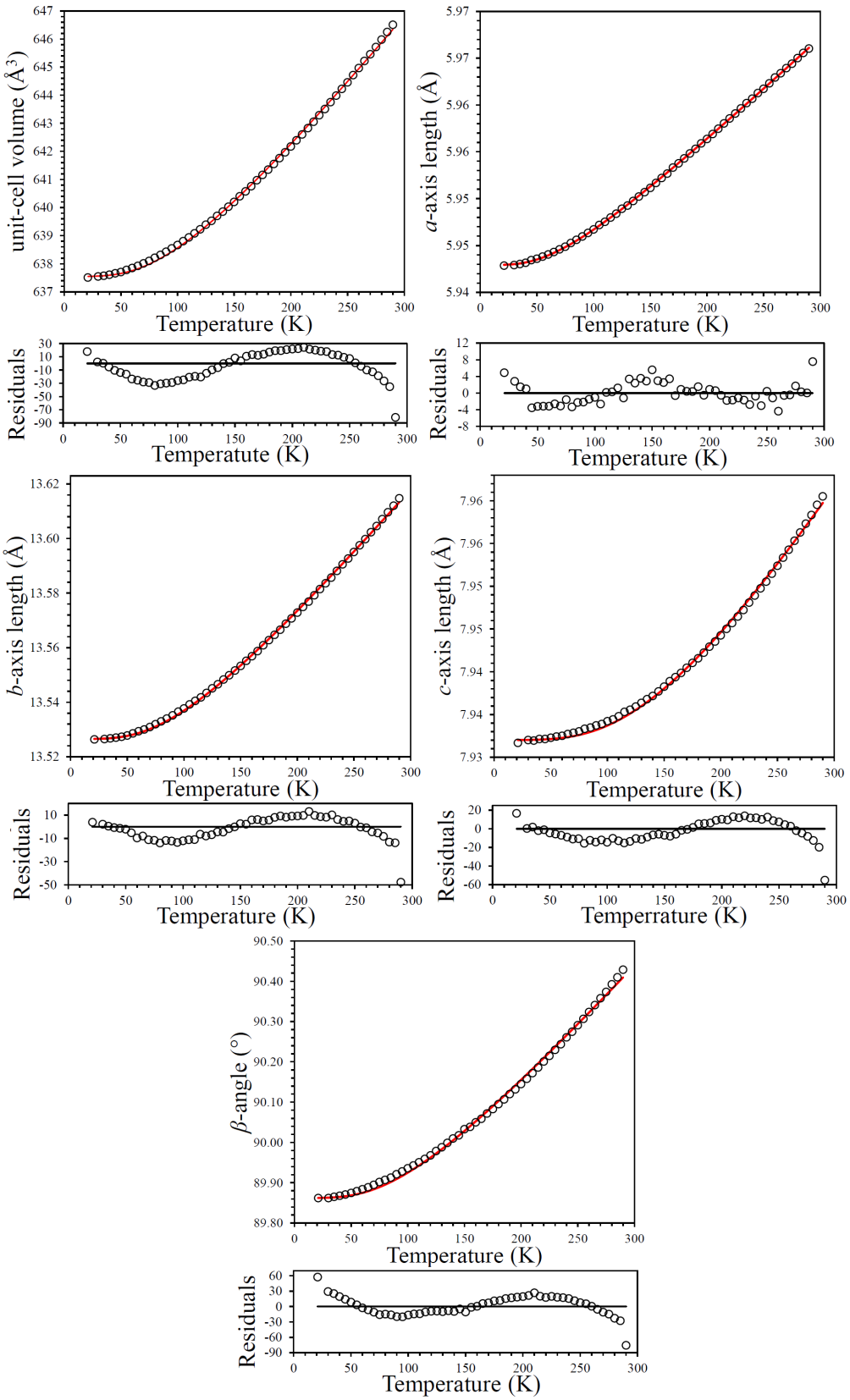

Fig. S2. First order Debye model fit (red line) upon the lattice parameters (black open circle) of rozenite at temperatures ranging from 290 to 21 K. Note the large residuals indicating the poor fit between the modelled and experimental data. Error bars are smaller than the symbol size.

	a^3 (Å^3)	b^3 (Å^3)	c^3 (Å^3)	β	V (Å^3)
θ_D (K)	267(2)	370(6)	610(15)	427(12)	379(8)
X_0 (cm^3 mol^{-1})	31.6002(4)	372.19(2)	75.192(3)	13.5307(3)	95.985(4)
X_0 (Å, Å^3)	5.9429(8)	13.5215(6)	7.9340(3)	89.873(21)	637.55(3)
Q (x10^4 J cm^{-3})	772(3)	404(4)	522(13)	1198(22)	560(7)
K_0/γ (GPa)	244.2(8)	10.9(1)	69(2)	885(16)	58.4(7)

Table S2. Parameters derived from fitting a first order single Debye model upon the lattice parameters of rozenite.

T (K)	*a* (Å)	*b* (Å)	*c* (Å)	*β* (°)	V (Å^3)
290	5.966031(12)	13.609756(31)	7.962529(14)	90.4288(2)	646.509(2)
280	5.965014(25)	13.604674(68)	7.960354(33)	90.3926(4)	645.984(4)
270	5.963939(24)	13.599606(68)	7.958306(33)	90.3580(4)	645.463(4)
260	5.962945(24)	13.594808(67)	7.956294(33)	90.3237(4)	644.967(4)
250	5.961745(24)	13.590061(67)	7.954417(33)	90.2914(4)	644.462(4)
240	5.960692(23)	13.585533(65)	7.952566(32)	90.2607(3)	643.986(4)
230	5.959640(24)	13.580734(69)	7.950936(32)	90.2295(4)	643.514(4)
220	5.958573(26)	13.576474(70)	7.949244(33)	90.2013(4)	643.061(4)
210	5.957480(25)	13.571914(66)	7.947720(32)	90.1724(3)	642.605(4)
200	5.956386(28)	13.567891(69)	7.946274(34)	90.1454(4)	642.181(4)
190	5.955319(29)	13.563782(69)	7.944954(34)	90.1195(4)	641.765(4)
180	5.954314(31)	13.559696(68)	7.943594(35)	90.0955(4)	641.355(4)
170	5.953319(28)	13.555902(63)	7.942473(32)	90.0719(4)	640.978(3)
160	5.952220(28)	13.551914(64)	7.941388(32)	90.0499(4)	640.584(3)
150	5.951150(26)	13.548306(63)	7.940260(32)	90.0329(6)	640.207(3)
140	5.950227(26)	13.544909(66)	7.939180(33)	90.0097(6)	639.860(3)
130	5.949275(27)	13.541560(66)	7.938362(33)	89.9884(6)	639.534(3)
120	5.948406(28)	13.538448(65)	7.937573(34)	89.9680(6)	639.230(3)
110	5.947544(30)	13.535534(67)	7.936811(35)	89.9512(5)	638.938(4)
100	5.946730(30)	13.532723(67)	7.936230(36)	89.9358(5)	638.671(4)
90	5.945970(32)	13.530188(71)	7.935726(38)	89.9208(4)	638.429(4)
80	5.945268(31)	13.528004(68)	7.935337(36)	89.9066(4)	638.219(4)
70	5.944600(30)	13.525946(69)	7.934868(36)	89.8951(4)	638.013(4)
60	5.944048(32)	13.524380(71)	7.934521(37)	89.8843(4)	637.851(4)
50	5.943604(32)	13.522808(74)	7.934297(37)	89.8749(4)	637.711(4)
40	5.943159(30)	13.522054(71)	7.934138(37)	89.8676(4)	637.615(4)
30	5.942915(33)	13.521509(75)	7.934013(38)	89.8622(4)	637.553(4)
21	5.942863(15)	13.521390(40)	7.933688(20)	89.8617(4)	637.516(2)

Table S3. Unit-cell parameters of rozenite determined upon cooling.

T (K)	*a* (Å)	*b* (Å)	*c* (Å)	β (°)	V (Å^3)
285	5.965567(26)	13.607071(74)	7.961536(35)	90.4097(4)	646.252(4)
275	5.964427(28)	13.602136(76)	7.959341(37)	90.3744(4)	645.719(4)
265	5.963399(26)	13.597331(75)	7.957339(36)	90.3408(4)	645.220(4)
255	5.962329(27)	13.592522(78)	7.955356(37)	90.3069(4)	644.717(4)
245	5.961293(26)	13.587664(77)	7.953491(36)	90.2753(4)	644.226(4)
235	5.960211(27)	13.583157(76)	7.951769(36)	90.2441(4)	643.757(4)
225	5.959095(27)	13.578656(73)	7.950095(35)	90.2145(4)	643.289(4)
215	5.958049(29)	13.574198(75)	7.948476(37)	90.1863(4)	642.835(4)
205	5.956920(30)	13.569922(75)	7.947025(37)	90.1581(4)	642.395(4)
195	5.955903(31)	13.565751(75)	7.945553(37)	90.1323(4)	641.970(4)
185	5.954832(32)	13.561609(73)	7.944251(37)	90.1070(4)	641.554(4)
175	5.953784(33)	13.557784(75)	7.943047(39)	90.0830(4)	641.163(4)
165	5.952678(34)	13.553785(74)	7.941882(39)	90.0594(5)	640.761(4)
155	5.951693(33)	13.550204(74)	7.940904(37)	90.0391(6)	640.407(4)
145	5.950715(31)	13.546632(75)	7.939709(38)	90.0184(7)	640.037(4)
135	5.949765(31)	13.543354(73)	7.938795(37)	89.9988(7)	639.706(4)
125	5.948936(31)	13.540089(75)	7.937936(38)	89.9786(7)	639.394(4)
115	5.947982(31)	13.536813(75)	7.937316(39)	89.9594(6)	639.087(4)
105	5.947203(31)	13.534176(76)	7.936431(40)	89.9427(5)	638.807(4)
95	5.946343(34)	13.531583(74)	7.935903(39)	89.9280(3)	638.550(4)
85	5.945606(37)	13.529043(76)	7.935487(42)	89.9129(4)	638.317(4)
75	5.944876(33)	13.526965(77)	7.935037(40)	89.9017(4)	638.104(4)
65	5.944305(35)	13.525010(78)	7.93472(41)	89.8893(4)	637.925(4)
55	5.943825(37)	13.523563(85)	7.934434(43)	89.8789(5)	637.782(4)
45	5.943449(34)	13.522385(80)	7.934136(40)	89.8709(4)	637.662(4)
35	5.943032(34)	13.521768(78)	7.933968(41)	89.8643(4)	637.574(4)

Table S4. Unit-cell parameters of rozenite determined upon heating.

Mode symmetry	Frequency (cm^{-1})	Mode symmetry	Frequency (cm^{-1})
A_g	63.55	A_g	590.21
B_g	71.65	B_g	598.23
A_g	90.82	A_g	614.41
B_g	98.75	B_g	616.26
A_g	99.07	A_g	671.79
A_g	114.29	B_g	678.32
B_g	120.61	A_g	685.36
B_g	122.76	B_g	732.51
A_g	145.93	A_g	746.82
B_g	157	B_g	752.27
B_g	163.46	A_g	773.02
A_g	167.96	B_g	794.41
A_g	173.36	A_g	805.91
B_g	180.99	B_g	808.76
B_g	189.95	A_g	822.09
A_g	192	B_g	828.89
B_g	198.37	B_g	840.79
A_g	201.07	A_g	849.33
A_g	205.75	B_g	882.62
B_g	206.56	A_g	897.78
A_g	211.67	A_g	908.4
B_g	212.98	B_g	909.93
B_g	226.19	B_g	942.54
A_g	228.06	A_g	945.5
A_g	233.17	A_g	995.73
B_g	237.02	B_g	997.65
B_g	247.07	A_g	1035.15
A_g	249.98	B_g	1039.11
B_g	257.95	A_g	1164.33
A_g	260.18	B_g	1188.61
A_g	271.78	A_g	1567.54
B_g	272.13	B_g	1579.04
B_g	283.17	A_g	1598.22
A_g	285.63	B_g	1603.92
A_g	358.26	B_g	1608.78
B_g	361.16	A_g	1611.26
B_g	397.28	B_g	1660.07
A_g	400.2	A_g	1660.65
B_g	411.81	A_g	3278.7
A_g	417.08	B_g	3282.4
B_g	423.51	A_g	3330.41
A_g	431.16	B_g	3333.83
A_g	447.93	A_g	3379.8
B_g	451.98	B_g	3394.08
A_g	457.45	B_g	3443.77
B_g	465.19	A_g	3444.63
A_g	480.06	A_g	3472.47

B_g	482.66	B_g	3473.16
B_g	502.88	A_g	3533.74
A_g	519.1	B_g	3533.93
A_g	566.21	A_g	3592.42
B_g	566.61	B_g	3595.6
A_g	573.74	A_g	3614.09
B_g	578.02	B_g	3635.25

Table S5. Frequency and symmetry of the computed Raman-active vibrational modes.

Mode symmetry	Frequency (cm^{-1})	Mode symmetry	Frequency (cm^{-1})
A_u	0	B_u	592.88
B_u	0	A_u	594.08
B_u	0	A_u	615.02
A_u	36.33	B_u	619.7
A_u	59.59	B_u	671.7
B_u	96.61	A_u	674.32
A_u	117.07	B_u	694.4
B_u	133.74	A_u	718.94
A_u	142.6	B_u	755.65
A_u	148.71	A_u	780.14
B_u	150.51	B_u	787.34
B_u	163.05	A_u	793.15
B_u	173.96	A_u	810.18
A_u	181.37	B_u	820.71
A_u	189.63	A_u	834.04
B_u	199.35	B_u	840.34
B_u	204.22	A_u	867.97
B_u	208.65	B_u	882.66
A_u	210.2	A_u	889.03
A_u	219.58	B_u	903.83
B_u	220.99	B_u	910.56
B_u	224.18	A_u	916.24
A_u	226.23	B_u	941.61
B_u	239.48	A_u	944.65
A_u	242.11	A_u	991.31
B_u	243.4	B_u	992.6
A_u	250.61	B_u	1040.96
A_u	260.34	A_u	1042.81
A_u	265.3	A_u	1156.67
B_u	266.62	B_u	1171.02
A_u	273.8	B_u	1554.51
B_u	277.02	A_u	1564.86
B_u	286.49	B_u	1582.68
A_u	302.53	A_u	1587.52
A_u	359.09	A_u	1600.93
B_u	359.93	B_u	1606.18
A_u	403.01	B_u	1611.6
B_u	403.22	A_u	1613.34
B_u	415.38	A_u	3288.4
A_u	418.25	B_u	3308.03
A_u	425.83	B_u	3344.71
B_u	429.31	A_u	3347.71
B_u	432	B_u	3377.25
A_u	441.42	A_u	3382.24
B_u	463.49	B_u	3468.65
A_u	472.3	A_u	3471.16

A_u	478.03	A_u	3472.67
B_u	478.38	B_u	3475.59
A_u	498.3	A_u	3540.06
B_u	506.08	B_u	3548.43
B_u	569.28	A_u	3592.14
A_u	569.44	B_u	3593.5
B_u	574.99	B_u	3611.45
A_u	575.76	A_u	3619.95

Table S6. Frequency and symmetry of the computed Infrared-active vibrational modes.